Egyptian Journal of Radiology and Nuclear Medicine

RESEARCH Open Access

Cardiac MRI T1 mapping and extracellular volume application in hypertrophic cardiomyopathy

Nahla D. Ali[1*], Noha Behairy[1], Ahmed Kharabish[1,2], Wesam Elmozy[1], Ahmed Yahya Hegab[3] and Samira Saraya[1]

Abstract

Background: Hypertrophic cardiomyopathy (HCM) is one of the commonest inheritable cardiac disorders. Being a global disease with diffuse myocardial fibrosis, it has a wide range of adverse outcomes ending with sudden cardiac death. Cardiac magnetic resonance (CMR) with late gadolinium enhancement (LGE) has become a reference standard for visualization of focal myocardial fibrosis. In the setting of less severe or more diffuse fibrosis, LGE is unlikely to reveal the presence of abnormal tissue given the lack of normal myocardium as a reference. Direct measurement of myocardial T1 time (T1 mapping) may improve these methodologic problems of LGE CMR in the setting of diffuse retention of gadolinium-based contrast material. So, we aim at this study to evaluate the clinical application of CMRI native and post-contrast T1 relaxation in assessing diffuse myocardial fibrosis non-invasively in hypertrophic cardiomyopathy.

Results: There was a significant difference between the percent of fibrosis detected by measuring the extracellular volume percent compared to that detected by LGE, with the former detecting fibrosis in 45.1% of the examined cardiac segments while the latter showed fibrosis in 20.9% of the cardiac segments. Also, measuring the native T1 values showed evidence of fibrosis in about 32.2% of the cardiac segments superseding the percent of fibrosis detected using the LGE alone. The ejection fraction percent showed a negative correlation with the left ventricular mass with a correlation coefficient value of − 0.139 where both interstitial and replacement fibrosis play an important role in the pathophysiology of diastolic dysfunction as well as impairing the myocardial contractility. Also, in cases of obstruction, the extracellular volume (ECV) is more likely to increase in the basal anterior and antero-septal segments as well as the basal inferior segment with *P* values 0.015, 0.013, and 0.045, respectively.

Conclusion: Diffuse fibrosis was found to be difficult to be distinguished using LGE. The unique ability of CMR to use proton relaxation times provides a quantitative measurement to detect increased interstitial volume in diffuse myocardial fibrosis. Moreover, it showed that in cases of obstruction, the segments exposed to the highest pressure are more vulnerable to the fibrotic process denoting a relationship between the pressure gradient and the adverse myocardial remodeling.

Keywords: T1 mapping, ECV (extracellular volume), HCM (hypertrophic cardiomyopathy), Myocardial fibrosis

* Correspondence: nahladeyaa@gmail.com
[1]Faculty of Medicine, Cairo University, Kasr El Aini St, Cairo, Egypt
Full list of author information is available at the end of the article

Background

Hypertrophic cardiomyopathy (HCM) is the commonest inheritable cardiac disorder, with an estimated prevalence of 1:500 in the general population. Its clinical manifestations are wide-ranging, including sudden cardiac death [1, 2]. It is also an extremely heterogeneous disease having several phenotypes with the most common of them is the asymmetric septal form [1, 3–6].

One of the serious findings in HCM patients is the marked increase in both interstitial and replacement fibrosis that may be patchy or diffuse [1, 7].

Structural abnormalities of the mitral valve are also characteristic in many HCM patients, such as increased leaflet area and secondary leaflet thickening [1, 3]. Systolic anterior motion (SAM) of the mitral valve is also common and is caused by the pressure drop in the narrowed left ventricular outflow tract (LVOT) leading to partial or complete outflow obstruction with moderate to severe mitral regurgitation [3].

Recently, MRI is established as a useful adjunct to transthoracic echocardiography in the diagnosis of HCM as well as identifying its phenotypes and assessing ventricular volumes, function and mass with detection of the hemodynamic compromises, and wall motion abnormalities in addition to its ability to assess myocardial fibrosis [2, 7–9].

Myocardial fibrosis is thought to contribute to sudden cardiac death, ventricular tachy-arrhythmias, left ventricular dysfunction, and heart failure [6, 10]. It is defined as a significant increase in the collagen volume fraction of myocardial tissue which in turn affects diastolic and subsequently systolic function [11].

Basically, 2 forms of myocardial fibrosis can be distinguished: interstitial fibrosis which is an increase in the interstitial volume fraction without a significant loss of cardiomyocytes, and replacement fibrosis which indicates the deposition of extracellular matrix to replace dead cardiomyocytes [12].

In most patients with overt HCM, dense focal fibrosis can be visualized non-invasively with the use of late gadolinium enhancement (LGE) and has been reported in up to 75% of HCM patients mostly as patchy midwall enhancement [2, 10].

However, diffuse myocardial fibrosis is more difficult to be distinguished using LGE since the myocardial signal intensity may be nearly isointense and may be globally nulled thus appearing to be a normal tissue [7, 13].

A unique feature of cardiac magnetic resonance (CMR) is its ability to use proton relaxation times, such as T1, to characterize myocardial tissue. These relaxation times can be quantified using recently created mapping sequences, which does not rely on an appropriate choice of the inversion time to achieve signal contrast but on a quantitative measurement and, therefore, also detects an increased interstitial volume when myocardial fibrosis is diffuse [11, 12]. Thus, the T1 map of the myocardium is a parametric reconstructed image, where each pixel's intensity directly corresponds to the T1 relaxation time of the corresponding myocardial voxel [11].

Recently, native T1 mapping has been shown as a promising new method for fibrosis assessment being a simpler, safer, and faster method avoiding contrast agent, high cost, and possibility of nephrogenic systemic fibrosis in patients with end-stage chronic kidney disease [14]. Previous studies in patients with HCM demonstrated that T1 relaxation times are significantly higher both in the hypertrophied segments and in the remote myocardium in comparison with healthy volunteers; it was also observed both in segments with and without LGE [14].

An improvement to the standard LGE technique involves a quantitative measurement of the T1 relaxation time after administration of the contrast agent. However, as the post-contrast T1 is affected by a variety of confounding factors, they are alone insufficient to reliably classify diseased and healthy tissues and unable to provide quantitative numbers on the amount of fibrosis [11].

The limitations of the single post-contrast T1 mapping technique can be overcome by a quantitative comparison of pre- and post-contrast T1 values of the myocardium and blood [11].

The myocardial extracellular volume (ECV) is measured as the percent of tissue composed of extracellular space. This topic is of current interest as a diagnostic tool for non-ischemic cardiomyopathies as well as for understanding aging processes [13].

We aimed at this study to evaluate the clinical application of CMRI native and post-contrast T1 relaxation in assessing diffuse myocardial fibrosis non-invasively in patients with hypertrophic cardiomyopathy.

Methods

- Institutional ethical clearance was taken before conducting this prospective study.
- Written consent was obtained from patients or their authorized representatives.
- Among a period of 13 months (from March 2018 to April 2020), 41 patients were referred to perform CMR after being diagnosed by echocardiography to confirm the diagnosis of HCM or for family screening.
- MRI was done to diagnose the presence of HCM, detect its phenotype, assess the presence of obstruction, and measure the gradient as well as assessing the presence of fibrosis using the routine LGE method and adding T1 mapping sequence to

evaluate its clinical application in assessing diffuse myocardial fibrosis non-invasively.

Inclusion criteria

- Patients diagnosed as or suspected to be HCM patients via echocardiography, family history, or electrocardiogram (ECG).

Exclusion criteria

- Patients with cardiac pacemakers, implantable hearing aids, intracranial metal clips, metallic bodies in the eye, insulin pumps, extreme claustrophobia, irregular heart rate, renal insufficiency (GFR< 30 ml/min/1.73 m^2), inability to sustain a breath-hold, morbid obesity, and clinically unstable patients.

CMR protocol

- Full clinical history with revision of previous laboratory data and cardiac investigations.
- Weight and height of the patients were assessed, and the patients were reassured and all steps were explained to them.

Image acquisition

- Examinations were performed using a 1.5-T scanner (Avanto, Siemens Medical Systems, Erlangen, Germany) with a master gradient system (45 mT/mpeak gradient amplitude, 200 m/T/s slew rate) and an eighteen-element array body surface coil and thirty-two element spine coil.
- Patients were put in the supine position, head first with ECG pads placed on the anterior chest wall.
- *Scout* images were taken followed by *cine* steady-state free precession (SSFP) images in 4-chamber, 2-chamber, short axis (SAX), 3-chamber, and LVOT planes. All images were acquired using retrospective gating during a gentle expiratory breath-hold; SAX cine images were acquired as a stack from the mitral valve plane through the apex covering the entire ventricles.
- *Phase-contrast flow images* were then acquired: first in in-plane view along the direction of blood flow followed by through-plane flow images (30 phases) centered on the aorta.
- *T1 quantification* was then performed with modified Look-Locker inversion recovery (MOLLI) sequence acquired pre- and 15 min following bolus contrast administration in 3 short-axis images (basal, mid-ventricular, and apical levels) with variable inversion preparation time, during the same cardiac phase at late diastole using the same imaging parameters. Typical acquisition parameters were as follows: echo time/repetition time = 1.03/413.57 ms, flip angle = 35°, field of view = 450 × 450 mm, matrix size = 256 × 169, interpolated pixel size = 1.8 × 1.8, GRAPPA = 2, 24 reference lines, cardiac delay time TD = 500 ms, 0.22-s acquisition time for a single image, and phase partial Fourier 7/8. The 5(3)3 MOLLI variant was used where two inversions were used, images acquired after first inversion 5, pause 3 heartbeats, and images acquired after second inversion 3.
- LGE images were obtained 6–10 min after intravenous injection of 0.15 mmol/kg body weight gadolinium contrast agent using inversion recovery prepared fast gradient echo sequence. Five minutes following contrast injection, TI scout was obtained to select the optimal inversion time for delayed enhancement imaging. Two-, 3-, and 4-chamber as well as SAX LGE images were performed covering the whole ventricle.

Image processing

- Three radiographers (5, 6, and 11 years of experience in cardiac MR imaging) interpret the images as being blind to the results of each other to reduce the bias.
- Using Argus (Siemens Healthcare, Erlangen, Germany), LV short-axis epicardial and endocardial borders were manually contoured at end-diastole and end-systole for determining EDV, ESV, SV, EF, and myocardial mass.
- Images were assessed to identify the *phenotype* of HCM, measure the *maximum wall thickness*, and identify its site.

For the evaluation of myocardial ECV, SAX T1 map images were assessed where a region of interest (ROI) > 12 pixels was drawn manually on the pre- and post-contrast images in each of the myocardial segments (according to the 17 segments' cardiac model) excluding the apex giving a total of 16 segments in each patient. ROI was also drawn in the blood pool in the pre- and post-contrast images. Those ROIs were drawn blindly without looking at the corresponding LGE images and were drawn carefully to avoid contamination and potential partial volume effects at the endo and epicardial borders (Fig. 1).

ECV was then calculated using the following equation:

$$\mathrm{ECV} = (1 - \text{hematocrit})\frac{(1 \div \text{T1 myo post}) - (1 \div \text{T1 myo pre})}{(1 \div \text{T1 blood post}) - (1 \div \text{T1 blood pre})}$$

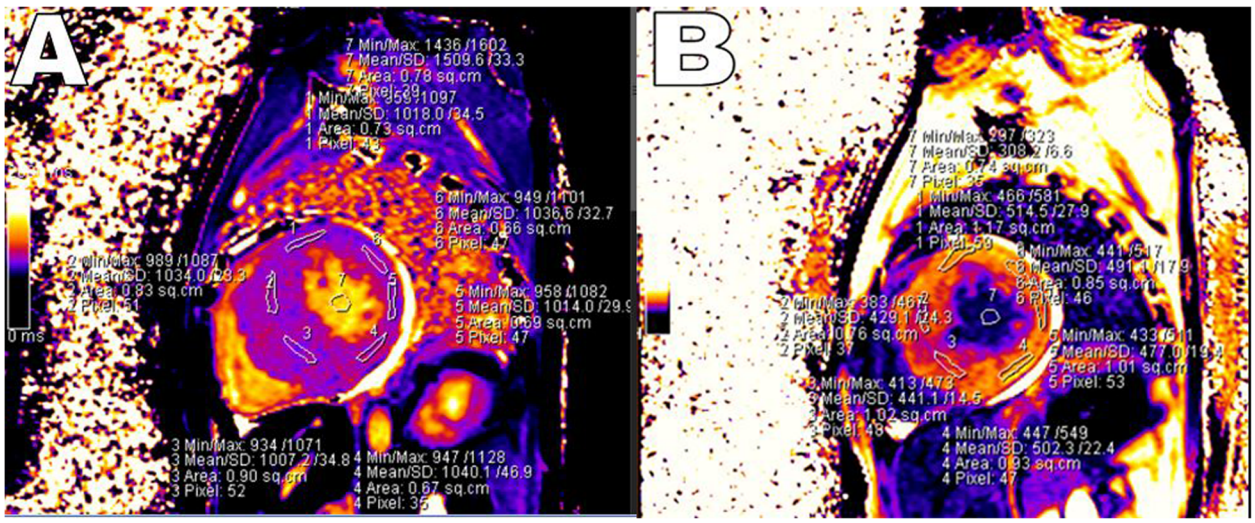

Fig. 1 Pre- (**a**) and post-contrast (**b**) T1 mapping images showing ROI drawn in the 6 basal segments: anterior, antero-septal, infero-septal, inferior, infero-lateral, and antero-lateral segments as well as the blood pool

- The ECV percent was considered expanded at 30% or more.
- Finally, the LGE images were checked at the different planes for the presence or absence of enhancement in each segment.
- Data were coded and entered using the Statistical Package for the Social Sciences version 24. Data was summarized using mean, standard deviation, median, and minimum and maximum for quantitative data and using frequency (count) and relative frequency (percentage) for categorical data. Comparisons between quantitative variables were done using the non-parametric Mann-Whitney test (Chan 2003a). For comparing the categorical data, the chi-square (× 2) test was performed. The exact test was used instead when the expected frequency is less than 5 (Chan 2003b). Correlations between quantitative variables were done using the Spearman correlation coefficient (Chan 2003c). *P* values less than 0.05 were considered statistically significant.

Results

This study included 29 males and 12 females, age range between 8 and 70 years with a median age of 45 years (Figs. 2, 3, and 4).

The phenotype

Among the study group, 26 (63.4%) patients had anteclockwise, 8 (19.5%) patients had septal, 4 (9.7%) patients had apical, 3 (7.3%) patients had asymmetric, and 2 (4.8%) patients had concentric patterns of hypertrophy

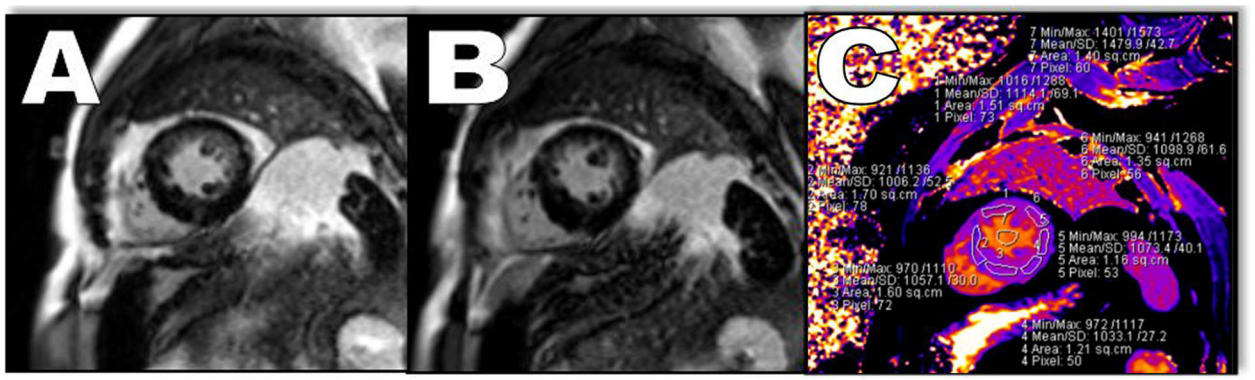

Fig. 2 a Mid-ventricular LGE image showing inferior insertion point enhancement and faint anterior and AL segment enhancement. **b** Mid-ventricular LGE at the same level of planned T1 mapping image showing faint focal inferior insertion point enhancement. **c** Native T1 mapping image planned at a different level from that showing enhancement

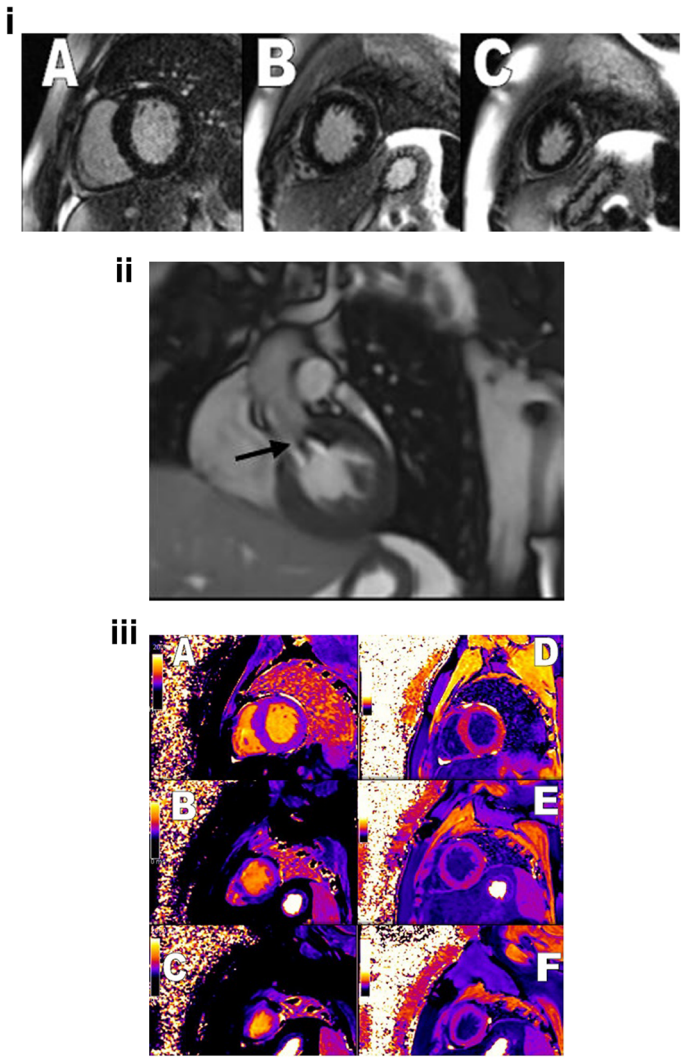

iv

	Basal ant	Basal AS	Basal IS	Basal inf	Basal IL	Basal AL	Mid ant	Mid AS	Mid IS	Mid inf	Mid IL	Mid AL	Apical ant	Apical sep	Apical inf	Apical lat
LGE	No LGE															
Native T1	949	981	993	987	988	929	1041	1045	1020	945	940	1034	961	919	916	1019
ECV	29%	31%	32%	33%	31%	27%	34%	32%	31%	23%	26%	30%	29%	26%	26%	33%

Fig. 3 Case 1: 26-year-old male patient. MRI showed asymmetric LV hypertrophy having anteclockwise pattern, maximum thickness of 17 mm affecting the basal antero-septal segment, LVOT obstruction with a peak velocity of 3 m/s, SAM and LV mass of 245 g (indexed 127 g/m^2). I: LGE images at the basal (**a**), mid-ventricular (**b**), and apical (**c**) levels corresponding to the T1 mapping cuts showing no significant enhancement. II: SSFP image in LVOT view showing candle flame artifact of LVOTO (arrow). III: pre-contrast (**a**–**c**) and post-contrast (**d**–**f**) T1 mapping images at the basal (**a**, **d**), mid-ventricular (**b**, **e**), and apical (**c**, **f**) levels. IV: enhancement pattern and values of native T1 and ECV at the basal, mid-ventricular, and apical segments showing no evidence of myocardial enhancement yet ECV expansion in 9 of the 16 cardiac segments

with two patients sharing two phenotypes giving a total of 43 phenotypic expression. Out of those patients, 12 (29.2%) patients had apical RV hypertrophy and 2 patients (4.8%) had LV apical aneurysm.

Volumes and function

Volumes and function are expressed in Table 1.

Percent of obstruction and correlating it to the ECV

Among the studied patients, 28 patients (68.3%) had hypertrophic obstructive cardiomyopathy (HOCM), while 13 patients (31.7%) had HCM without obstruction. Correlating the ECV to the presence of obstruction, the results were statistically significant in the basal anterior and antero-septal segments (those are

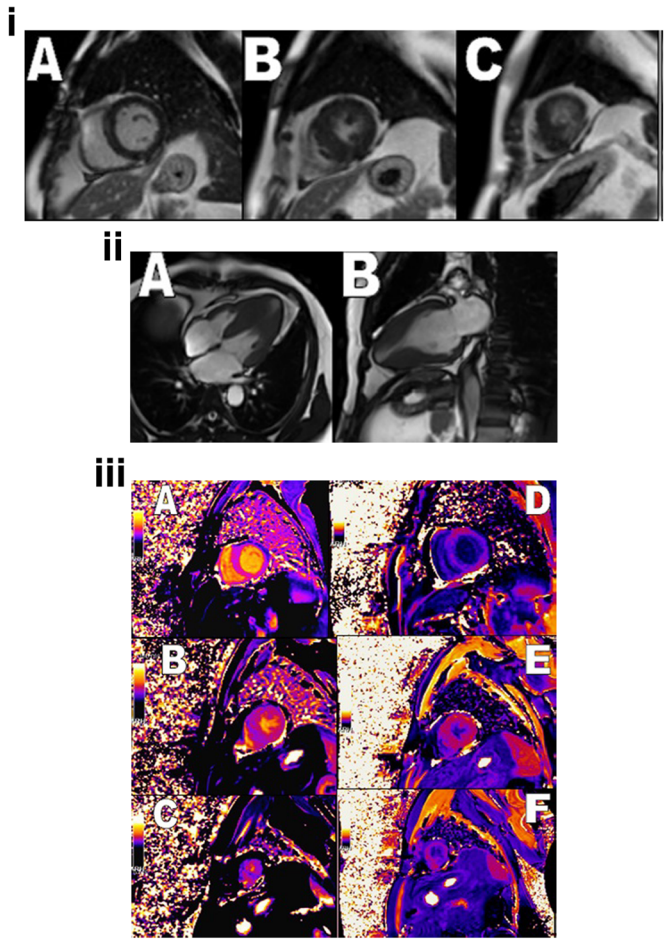

iv

	Basal ant	Basal AS	Basal IS	Basal inf	Basal IL	Basal AL	Mid ant	Mid AS	Mid IS	Mid inf	Mid IL	Mid AL	Apical ant	Apical sep	Apical inf	Apical lat
LGE		faint	Insert.												patchy	patchy
Native T1	1036	1104	1163	1170	1051	1026	1089	1066	1043	1125	1109	1100	1068	1076	1071	1081
ECV	29%	41%	41%	34%	37%	38%	30%	34%	32%	32%	34%	30%	36%	32%	44%	36%

Fig. 4 Case 2: 51-year-old male patient. MRI showed LV hypertrophy having apical distribution, mild RV hypertrophy, maximum thickness of 20 mm affecting the apical segments, mid-cavitary obstruction with LV mass of 189 g (indexed 106 g/m^2). I: LGE images at the basal (**a**), mid-ventricular (**b**), and apical (**c**) levels corresponding to the T1 mapping cuts showing faint basal AS segment and inferior insertion point enhancement and patchy enhancement of the apical inferior and lateral segments. II: SSFP images in 4-chamber (**a**) and 2-chamber (**b**) end-systolic views showing mid-ventricular to apical hypertrophy with mid-cavitary obstruction. III: pre-contrast (**a**–**c**) and post-contrast (**d**–**f**) T1 mapping images at the basal (**a**, **d**), mid-ventricular (**b**, **e**), and apical (**c**, **f**) levels. IV: enhancement pattern and values of native T1 and ECV at the basal, mid-ventricular, and apical segments showing the expansion of the ECV and elongation of the native T1 values not only in the segments showing enhancement but in other segments as well

exposed to the highest pressure), as well as the basal inferior segments with P values of 0.015, 0.013, and 0.045, respectively.

Correlating the ECV to the presence of LGE

LGE was noted in 20.9% of the cardiac segments, while ECV expansion was noted in 45.1% of the cardiac segments.

Of those segments that showed LGE, only 79.6% showed ECV expansion while the rest of the segments (20.4%) representing 4.3% of the entire cardiac segments did not show ECV expansion. On the other hand, 28.5% of the cardiac segments showed ECV expansion with no evident LGE.

Correlating the native T1 value to the ECV

There was elongation of the native T1 value in 32.3% of the cardiac segments while ECV expansion in 45.1% of the segments. However, the P values were < 0.05 in 5

Table 1 Left and right ventricular volumes and functions among the study group

	Mean	Standard deviation	Median	Minimum	Maximum
LV EF	66.10	10.53	68.00	35.00	84.00
LV EDV	156.22	48.81	154.00	76.00	295.00
LV ESV	54.78	28.81	50.00	18.00	144.00
LV SV	101.39	30.17	98.00	49.00	192.00
LV EDVI	86.54	24.45	82.00	40.00	176.00
LV ESVI	32.39	18.95	28.00	14.00	110.00
LV SVI	55.27	17.22	54.00	18.00	114.00
LV mass	223.49	95.54	212.00	85.00	493.00
RV EF	67.78	10.69	70.00	27.00	82.00
RV EDV	122.76	32.69	118.00	81.00	194.00
RV ESV	40.63	22.86	36.00	18.00	137.00
RV SV	82.12	22.50	78.00	38.00	150.00
RV EDVI	67.73	15.90	66.00	40.00	106.00
RV ESVI	22.49	11.41	20.00	9.00	65.00
RV SVI	45.34	10.49	46.00	18.00	66.00

basal segments, 4 mid-ventricular level segments, and 2 apical segments with a linear regression curve proving that as the native T1 value increases, the probability of fibrosis increases. In the basal segments, it was found that at native T1 values 950, 1000, 1100, and 1200 ms, the probability of fibrosis was 14%, 26%, 65%, and 90%, respectively.

Correlating the native T1 values to the presence of LGE

We had elongation of the native T1 values in 32.2% of the segments while LGE in 20.9% of the cardiac segments. Sixty-two percent of the segments that showed LGE showed native T1 elongation. Of the entire cardiac segments, 9.7% showed LGE without evidence of native T1 elongation, while there was elongation of the T1 in 19.4% of segments without evidence of enhancement.

Correlating the EF% to the LV mass

A negative correlation with a correlation coefficient of −0.139 was found.

Discussion

Hypertrophic cardiomyopathy is the most common heritable cardiovascular disorder, with myocardial fibrosis being one of its hallmarks [10].

MRI has recently become an important tool for the evaluation of suspected HCM. It can also be used as a guide for suitable therapy, risk stratification, and family screening tool [2, 5].

CMR can detect regional fibrosis by LGE but in diffuse fibrotic processes defining an area of normal myocardium to be a nulled reference may be impossible [15].

Consequently, several studies have proposed the measurement of T1 relaxation as a potentially valuable tool for the quantitative assessment of myocardial fibrosis [15].

Regarding the phenotype of HCM, the results agree with Bogaert and Olivotto [3], who stated that "In a recent analysis of the spatial 3D spread of hypertrophy, we found that the majority of patients with so-called asymmetrical septal HCM follow a spiral pattern of hypertrophy in longitudinal direction following a counterclockwise spiral, when viewed from LV apex."

However, Noureldin et al. [1] stated that the asymmetric phenotype with sigmoid septal contour is the commonest phenotype, and Hoey et al. [2] stated that the asymmetric septal type is the commonest phenotype. This difference is most likely attributed to the lack of overall 3D look on the LV, where in the counterclockwise pattern, the most hypertrophied segment is usually the anteroseptal basal segment; however, the overall pattern of hypertrophy is spiral in an anteclockwise fashion when viewed from the cardiac apex.

Regarding the RV hypertrophy, the results are not far from Hoey et al. [2] who stated that 15–20% of HCM patients have associated RV hypertrophy. However, Noureldin et al. [1], said that RV hypertrophy is present in approximately 18% of HCM patients.

The results regarding the prevalence of obstruction among HCM patients agreed with Hoey et al. [2] who said that LVOT obstruction is present in up to 70% of HCM patients and Noureldin et al. [1] who stated that asymmetric septal hypertrophy with sigmoid septal contour is the commonest phenotype accounting for about two thirds of HCM patients and is associated with obstruction.

Regarding the ECV, the current study proved that it has a better predictive value for fibrosis than the LGE, through correlating the ECV with LGE.

This agrees with Kellman et al. [13], who stated that ECV mapping is a promising technique complementing LGE imaging in cases of diffuse myocardial disease states. Also, Taylor et al. [16] and Lu et al. [15] stated that the T1 mapping technique has enabled better, non-invasive evaluation of the extent and severity of myocardial fibrosis compared to the conventional LGE technique to a level that was previously achieved with invasive procedures such as cardiac biopsy.

The results for correlating the ECV to the native T1 values and the native T1 values to the LGE were in agreement with Dass et al. [17], who stated that T1 mapping is more efficient in detecting myocardial changes in patients with cardiomyopathies compared to the traditional ways of measuring the myocardial wall thickness and LGE. Also, Sibley et al. [18] stated that T1 time correlates with interstitial fibrosis in patients with cardiomyopathy including those without focal LGE.

However, Puntmann et al. [19] stated that native T1 has a better diagnostic accuracy than post-contrast T1 values and ECV. This could be due to the small sample size and the blind quantification of T1 without checking the LGE images. And that agrees with Nezafat [20] who conducted a study on ischemic patients and stated that visual detection of infarct on native T1 maps was only moderate (low 60%).

Regarding the relation of the EF% to the LV mass, we had a negative correlation indicating that as the mass of the left ventricle increases, the EF% decreases.

This agrees with Taylor et al. [16] who stated that diffuse fibrosis may play an important role in the pathophysiology of diastolic dysfunction where reduced LV ejection fraction is correlated to the increase of ECV in patients with non-ischemic cardiomyopathy. And as HCM patients have both interstitial and replacement fibrosis, therefore, the myocardial contractility is as well affected [1, 11].

Correlating the ECV to the presence and absence of obstruction, the results were of statistical significance in the basal anterior and antero-septal segments as well as the basal inferior segments, denoting that there is a positive relation between the expansion of the ECV at those segments and the presence of obstruction, knowing that in cases of left ventricular outflow obstruction, there is always hypertrophy of the basal anterior and antro-septal segments and those are the segments exposed to the maximum pressure. Similar findings were reported by Ooji et al. [21] who mentioned that there is a structure-function relationship between elevated LVOT pressure gradient and adverse myocardial remodeling.

The limitations of this study include the following: (1) The ECV expansion was considered at values ≥ 30% taking the published range of normal ECV value of 20–30% as a reference, while some papers consider the normal up to 25.3 ± 3.5% and others consider it as 25.4 ± 2.5%. (2) The ROIs were drawn blindly without checking the LGE images, to check the validity of T1 as a tool to replace LGE. (3) Some segments showed enhancement at one cut while the T1 mapping cut was planned at a different level from that showing enhancement. Those factors may attribute to the absence of ECV expansion in some segments that showed LGE where some segments showed focal insertion point enhancement and others showed subendocardial enhancement, while the T1 mapping ROI was drawn at the proper segment location.

Conclusion

Diffuse fibrosis was found to be difficult to be distinguished using LGE. The unique ability of CMR to use proton relaxation times provides a quantitative measurement to detect increased interstitial volume in diffuse myocardial fibrosis. Moreover, it showed that in cases of obstruction, the segments exposed to the highest pressure are more vulnerable to the fibrotic process denoting a relationship between the pressure gradient and the adverse myocardial remodeling.

Abbreviations

CMR(I): Cardiac magnetic resonance (imaging); ECG: Electrocardiogram; ECV: Extracellular volume; EDV(I): End-diastolic volume (indexed); EF: Ejection fraction; ESV(I): End-systolic volume (indexed); GFR: Glomerular filtration rate; HCM: Hypertrophic cardiomyopathy; IR: Inversion recovery; LGE: Late gadolinium enhancement; LV: Left ventricle; MI: Myocardial infarction; MOLLI: Modified look locker; MRI: Magnetic resonance imaging; RV: Right ventricle; SAPPHIRE: Saturation pulse prepared heart rate independent inversion recovery; SASHA: Saturation recovery single-shot acquisition; ShMOLLI: Shortened modified look locker; SSFP: Steady-state free precession; SV(I): Stroke volume (indexed)

Acknowledgements

Not applicable.

Authors' contributions

NDA, NB, AK, WEM, and SS reviewed all the patients' magnetic resonance images. NDA analyzed and interpreted the patient data and wrote the manuscript. All authors read and approved the final manuscript.

Funding

Not applicable (no funding was provided).

Availability of data and materials

The datasets used and/or analyzed during the current study are available from the corresponding author on reasonable request.

Ethics approval and consent to participate

- Institutional (*Faculty of Medicine "Kasr El-Ainy Hospital," Cairo University*) ethical clearance was taken before conducting this prospective study; March 2016—reference number: not available.
- Written consent was obtained from patients or their authorized representatives.

Consent for publication
All patients included in this research gave written informed consent to publish the data contained within this study. If the patient was less than 16 years old, deceased, or unconscious when consent for publication was requested, written informed consent for the publication of this data was given by their parent or legal guardian.

Competing interests
The authors declare that they have no competing interests.

Author details
[1]Faculty of Medicine, Cairo University, Kasr El Aini St, Cairo, Egypt. [2]Radiology Department, Liverpool Heart and Chest Hospital, Liverpool, UK. [3]National Heart Institute, Cairo, Egypt.

Received: 13 August 2020 Accepted: 17 January 2021
Published online: 18 February 2021

References

1. Noureldin RA, Liu S, Nacif MS, Judge DP, Halushka MK, Abraham TP, Ho C, Bluemke DA (2012) The diagnosis of hypertrophic cardiomyopathy by cardiovascular magnetic resonance. JCMR. 14:17
2. Hoey ETD, Elassaly M, Ganeshan A, Watkin RW, Simpson H (2014) The role of magnetic resonance imaging in hypertrophic cardiomyopathy. Quant Imaging Med Surg 4(5):397–406
3. Bogaert J, Olivotto I (2014) MR imaging in hypertrophic cardiomyopathy: from magnet to bedside. Radiol. 273:2
4. Parato VM, Antoncecchi V, Sozzi F, Marazia S, Zito A, Maiello M, Palmiero P (2016) Echocardiographic diagnosis of the different phenotypes of hypertrophic cardiomyopathy. Cardiovasc Ultrasound. 14:30
5. Koshy M, Johari B, Hamdan MF, Hanafiah M (2016) Role of cardiac MRI in detecting familial hypertrophic cardiomyopathy: review. JCHS. 1:4–9
6. Marian AJ, Braunwald E (2017) Hypertrophic cardiomyopathy genetics, pathogenesis, clinical manifestations, diagnosis, and therapy. Circ. 121:7
7. Haaf P, Garg P, Messroghli DR, Broadbent DA, Greenwood JP, Plein S (2016) Cardiac T1 mapping and extracellular volume (ECV) in clinical practice: a comprehensive review. J Cardiovasc Magn Reson 18:89
8. Geske JB, Ommen SR, Gersh BJ (2018) Hypertrophic cardiomyopathy clinical update. JACC 6:5
9. Habib M, Hoss S, Rakowsk H (2019) Evaluation of hypertrophic cardiomyopathy: newer echo and MRI approaches. Curr Cardiol Rep 21:75
10. Ho CY, López B, Coelho-Filho OR, Lakdawala NK, Cirino AL, Jarolim P, Kwong R, González A, Colan SD, Seidman JG, Díez J, Seidman CE (2010) Myocardial fibrosis as and early manifestation of hypertropic cardiomyopathy. N Engl J Med 363:552–563
11. Perea RJ, Ortiz-Perez JT, Sole M, Cibeira MT, de Caralt TM, Prat-Gonzalez S, Bosch X, Berruezo A, Sanchez M, Blade J (2015) T1 mapping: characterisation of myocardial interstitial space. Insights Imaging. 6:189–202
12. De Graaf WL, Vandoorne K, Arslan F, Nicolay K, Strijkers GJ (2014) Contrast-enhanced T1-mapping MRI for the assessment of myocardial fibrosis. Curr Cardiovasc Imaging. 7:9260
13. Kellman P, Wilson JR, Xue H, Ugander M, Arai1AE (2012) Extracellular volume fraction mapping in the myocardium, part 1; evaluation of an automated method. JCMR. 14:63
14. White SK, Sado DM, Fontana M, Banypersad SM, Maestrini V, Flett AS, Piechnik SK, Robson MD, Hausenloy DJ, Sheikh AM, Hawkins PN and Moon JC (2013) T1 mapping for myocardial extracellular volume measurement by CMR. JACC. 955 – 62(11)
15. Lu M, Zhao S, Yin G, Jiang S, Zhao T, Chen X, Tian L, Zhang Y, Wei Y, Liu Q, He Z, Xue H, An J and Shah S (2013) T1 mapping for detection of left ventricular myocardial fibrosis in hypertrophic cardiomyopathy: a preliminary study. European Journal of Radiology. e225– e231 (13)
16. Taylor AJ, Salerno M, Dharmakumar R, Jerosch-Herold M (2016) T1 mapping. JACC 9:1 (14)
17. Dass S, Suttie JJ, Piechnik SK, Ferreira VM, Holloway CJ, Banerjee R, Mahmod M, Cochlin L, Karamitsos TD, Robson MD, Watkins H, Neubauer S (2012) Myocardial tissue characterization using magnetic resonance noncontrast T1 mapping in hypertrophic and dilated cardiomyopathy. Circ Cardiovasc Imaging. 5:726–733(15)
18. Sibley CT, Noureldin RA, Gai N, Nacif MS, Liu S, Evrim B, Turkbey EB, Mudd JO, Van der Geest RJ, Lima JAC, Halushka MK, Bluemke DA (2012) T1 mapping in cardiomyopathy at cardiac MR: comparison with endomyocardial biopsy. Radiology 265:3(16)
19. Puntmann VO, Voigt T, Chen Z, Mayr M, Karim R, Rhode K, Pastor A, Carr-White G, Razavi R, Schaeffter T and Nagel E (2013) Native T1 mapping in differentiation of normal myocardium from diffuse disease in hypertrophic and dilated cardiomyopathy. JACC. 475–84.(12)
20. Nezaraft R (2015) Native T1 mapping for myocardial infarction. JACC. 8:9(17)
21. Ooij PV, Allen BD, Contaldi C, Garcia J, Collins J, Carr J, Choudhury L, Bonow RO, Barker AJ, Markl M (2016) 4D flow MRI and T1-mapping: assessment of altered cardiac hemodynamics and extracellular volume fraction in hypertrophic cardiomyopathy. J. Magn. Reson. Imaging. 43:107–114(18)

Publisher's Note